Advances in Biomechanics and Applications, *Vol. 1, No. 4 (2014) 253-267*
DOI: http://dx.doi.org/10.12989/aba.2014.1.4.253

On the properties of brain sub arachnoid space and biomechanics of head impacts leading to traumatic brain injury

Parisa Saboori[1a] and Ali Sadegh[*2]

[1]*Department of Mechanical Engineering, Manhattan College, Manhattan College Parkway, Riverdale, New York, USA*
[2]*Department of Mechanical Engineering, The City College of the City University of New York, 160 Convent Ave, New York, USA*

(Received April 15, 2014, Revised November 15, 2014, Accepted February 24, 2015)

Abstract. The human head is identified as the body region most frequently involved in life-threatening injuries. Extensive research based on experimental, analytical and numerical methods has sought to quantify the response of the human head to blunt impact in an attempt to explain the likely injury process. Blunt head impact arising from vehicular collisions, sporting injuries, and falls leads to relative motion between the brain and skull and an increase in contact and shear stresses in the meningeal region, thereby leading to traumatic brain injuries. In this paper the properties and material modeling of the subarachnoid space (SAS) as it relates to Traumatic Brain Injuries (TBI) is investigated. This was accomplished using a simplified local model and a validated 3D finite element model. First the material modeling of the trabeculae in the Subarachnoid Space (SAS) was investigated and validated, then the validated material property was used in a 3D head model. In addition, the strain in the brain due to an impact was investigated. From this work it was determined that the material property of the SAS is approximately E = 1150 Pa and that the strain in the brain, and thus the severity of TBI, is proportional to the applied impact velocity and is approximately a quadratic function. This study reveals that the choice of material behavior and properties of the SAS are significant factors in determining the strain in the brain and therefore the understanding of different types of head/brain injuries.

Keywords: brain; subarachnoid space properties; material modeling; impact; TBI

1. Introduction

Traumatic Brain Injury (TBI), which is mainly due to vehicular collisions, contact sports or falls, has a high incidence rate of fatal and nonfatal hospitalizations. The average number of such injuries in the US is approximately 175 to 200 per 100,000 according to the CDC (2011). TBIs are generally caused by contact (blunt head impacts) or non-contact (linear and/or angular accelerations) of the head which in either case causes relative motion between the brain and the skull. This increases the normal and shear stresses in the skull/brain interface region. The human brain is encased in the skull and is suspended and supported by a series of fibrous tissue layers,

∗Corresponding author, Ph.D., E-mail: sadegh@ccny.cuny.edu
[a]Ph.D., E-mail: parisa.saboori@manhattan.edu

 ISSN: 2287-2094 (Print), 2287-2272 (Online)

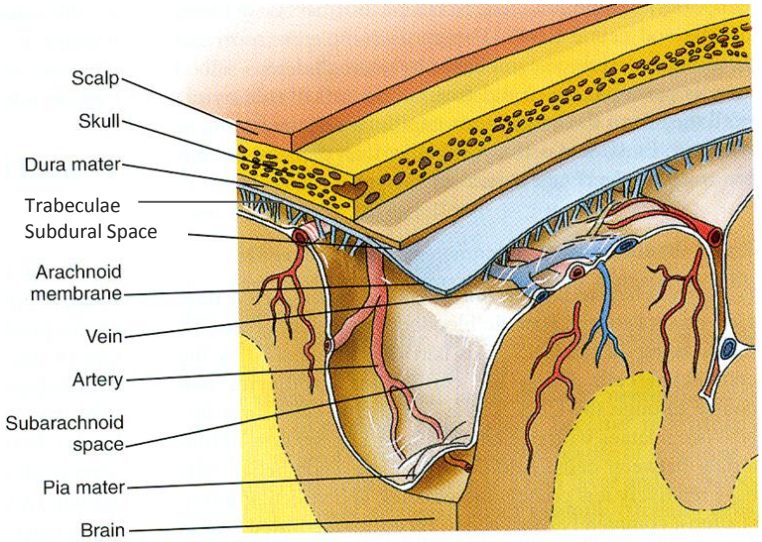

Fig. 1 Schematic diagram of the SAS space, trabeculae, the pia mater and the arachnoid. Photo. 18 June. 2013 <http://web.as.uky.edu/>

dura mater, arachnoid, trabeculae and pia mater, known as the meninges Fig. 1. In addition, cerebrospinal fluid (CSF), located in the space between the arachnoid and the pia mater which is known as the subarachnoid space (SAS), stabilizes the shape and the position of the brain during head movements. The cellular component of the pia, arachnoid, and the trabeculae and septae of the subarachnoidal space are meningothelial cells (MECs). Meningothelial cells (MECs) are the cellular components of the meninges which provide an important barrier function for the central nervous system (CNS) building the interface between neuronal tissue and the cerebrospinal fluid (CSF), and are also part of the immune response of the CNS, Jia *et al*. (2014). Consequently, the SAS damps and reduces the relative motion of the brain with respect to the skull. However, the mechanical properties of the meningeal layer, and in particular the trabeculae, are not well established in the literature.

The trabeculae in the SAS are known to have the form of rods (fibers) and thin transparent plates extending from the arachnoid (subdural) to the pia mater, Killer *et al*. (2003, 2006). The pia mater adheres to the surface of the brain and follows all its contours including the folds of the cerebral and cerebellar cortices. This gives the subarachnoid space a highly irregular shape and makes the distribution of CSF around the brain non-uniform. The volume of CSF is highest within the cisterns regions of the brain where, due to the shape of the brain surface, the subarachnoid space is largest. The arachnoid trabeculae are more concentrated in the subarachnoid cisterns, sometimes even coalescing into membranes that partially occlude the subarachnoid space, Saboori (2011), Saboori and Sadegh (2014). This correlation between the CSF and the trabeculae suggests that their functions are not independent. These fluid and solid phases work together to mechanically support the brain and damp its movement. Therefore, the SAS plays an important role in damping the brain motion and transferring blunt impacts to the brain.

Experimental, analytical, and numerical methods -and in particular finite element (FE) methods- have been employed by investigators to explain the likely injury process of the brain and to quantify the response of the human head to blunt impacts (Al-Bsharat *et al.* 1999, Drew 2004,

Jin *et al.* 2006, Kleiven and Hardy 2002, Rao and Lyketsos 2000, Ruan *et al.* 1993, Sabet *et al.* 2007, Zhang *et al.* 2001b, Zhang *et al.* 2002, Zoghi and Sadegh 2010). The complicated geometry of the SAS and trabeculae makes it impossible to model all the details of the region, Kierszenbaum (2007) and Killer *et al*. (2006). Thus, in these studies and other similar studies, the meningeal layers and the subarachnoid region have been simplified as a soft elastic material or in some cases as water (i.e., a soft solid having the bulk modulus of water and a very low shear modulus), Guo *et al.* (2000), Jin *et al.* (2006), Zhang *et al.* (2001b), Zhang *et al.* (2002). The shortcoming of these approaches is that the hydraulic damping (i.e., the fluid solid interaction) and the mechanical role of the fibrous trabeculae and the cerebrospinal fluid (CSF) in the subarachnoid space (SAS) were ignored. In addition to the simplified models, the mechanical properties of the SAS have not been well established in the literature. There have been wide ranges of Young's moduli for the Pia Arachnoid Complex (PAC) from 21.5×10^6 Pa reported by Zhang *et al.* (2001b) to 59×10^3 Pa reported by Jin *et al.* 2006, which is an up to three order of magnitude variation. In the study of Zoghi and Sadegh (2009), the damping characteristics of the SAS region were determined using the experimental study of Hardy *et al.* (1977). This was done by determining the damping coefficient of the brain/skull system and relating it to the hydraulic resistance of the CSF in the SAS region. Therefore, the material property of the SAS, as an interface between the skull and the brain, was identified to significantly affect the mechanotransduction of the external load to the brain.

To estimate the material property of the SAS in this study, two steps were taken. In the first step the range of the material properties of the trabeculae, as reported in the literature, was analyzed using a 2D transverse model of the head and the optimum value of the elastic moduli of the SAS was examined. The result of the model was compared and validated using the experimental study of Sabet *et al.* (2007) and the material property of the SAS was thereby determined. It has been shown that the material properties of the meningeal layer are significant factors in determining the strain in the brain and therefore understanding the different types of brain/head injuries. To simulate the function of trabeculae and the motion of the brain with respect to the skull in a more global sense a 3D head model was generated and validated. Finally, the strains in the brain due to the transmission of impact loads from the skull to the brain were investigated. The results indicate that the strain in the brain is quadratically proportional to the impact speed, and therefore to different types of TBI.

2. Materials and methods

The histology and architecture of SAS trabeculae have not been fully addressed in the literature, Schachenmayr and Friede (1978). Killer *et al.* (2003) studied the structure of trabeculae in the human optic nerve and it was found that the structure of the trabeculae depends on the location within the different portions of the optic nerve. It was also concluded that the SAS of the human optic nerve is not a homogeneous media and it contains a complex system of arachnoid trabeculae, septa, and pillars. In experimental histological studies, Saboori and Sadegh (2009), Saboori and Sadegh (2010), and Saboori (2011), it was reported that similar pillars and septa morphology describe the architecture of the SAS in rat brains.

In addition, the material structure of the collagen that makes up the SAS trabeculae has not been fully investigated. Some researchers reported that the trabeculae are soft tissue containing 50% collagen (Type I and IV) and 50% water, Feng *et al.* (2010). It has also been observed that in

the absence of CSF, the trabeculae are collagen Type I and they collapse since they are made of a very soft tissue (i.e., trabeculae buckle under compressive loads, Saboori and Sadegh 2010).

Equally, the mechanical properties of the SAS have not been established in the literature. Specifically, the stated Young's moduli for the Pia Arachnoid Complex (PAC) vary from 21.5×10^6 Pa reported by Zhang *et al.* (2001b) to 59×10^3 Pa reported by Jin *et al.* (2006) which is a three order of magnitude range. In this section the reported range of material properties is examined using a 2D and a 3D models, and an optimum value for the modulus of elasticity of the SAS is presented.

2.1 2D transverse model of the head

A two-dimensional transverse model of the head of an adult female patient in her 50's was created using the magnetic resonance imaging (MRI) images of her head (Fig. 2(a)). The corresponding finite element model Fig. 2(a) consists of the scalp, skull, dura mater, SAS, and the brain Fig. 2(b). A range of elastic moduli for the SAS was used in the model and was compared to the experimental results of Sabet *et al.* (2007) and Bayly *et al.* (2005).

In this part of the study ABAQUS/CAE 6.9-2 was used as a preprocessor; the details of the geometry and the dimensions were determined using eRAD/Image Medical Practice builder 1-2-3 software and were imported into the ABAQUS sketch module. The model was then meshed using quadratic linear elements. The input boundary condition for the study was taken from an experimental study by Sabet *et al*. (2007), where a mild angular acceleration was applied to three

Table 1 Material properties used for the models

Skull	Young's modulus, E (Pa)	12.2×10^9
	Poisson's ratio, υ	0.22
	Density, ρ(kg/m^3)	2.12×10^3
Dura mater	Young's modulus, E (Pa)	31.5×10^6
	Poisson's ratio, υ	0.45
	Density, ρ(kg/m^3)	1.13×10^3
Arachnoid and trabeculae (First analysis [10] and 12 cases for the range of E)	Young's modulus, E (Pa)	59.8×10^3 Range: 10^2 to 10^5
	Poisson's ratio, υ	0.49
	Density, ρ(kg/m^3)	1.13×10^3
Arachnoid and trabeculae (second analysis determined by this study)	Young's modulus, E (Pa)	1.15×10^3
	Poisson's ratio, υ	0.49
	Density, ρ(kg/m^3)	1.13×10^3
Muscles	Young's modulus, E (Pa)	1.0×10^7
	Poisson's ratio, υ	0.38
	Density, ρ(kg/m^3)	1.01×10^3
Neck	Young's modulus, E (Pa)	6.04×10^9
	Poisson's ratio, υ	0.38
	Density, ρ(kg/m^3)	1.18×10^3

Jin *et al.* (2006) and Takhounts *et al.* (2008)

Table 2 Tissue material properties of the brain as a linear viscoelastic model, used in this study

Brain tissue	
Shear modulus at t=0, G_0(Pa)	10.0×10^3
Shear modulus at t=∞, G_∞(Pa)	2.0×10^3
Bulk modulus at t=0, K_0(Pa)	5.0×10^7
Bulk modulus at t=∞, K_∞(Pa)	5.0×10^7
Relaxation time, λ (s^{-1})	16
Density, ρ(kg/m^3)	1.04×10^3

Takhounts *et al.* (2008)

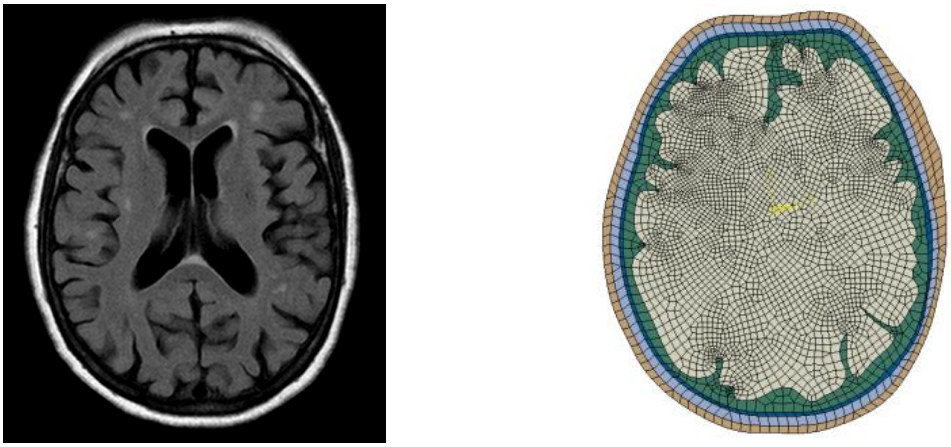

(a) (b)

Fig. 2 The MRI image of the transverse plane of; (a) a human head; and (b) the corresponding FE model

human subjects and the resulting strains in the brain were measured. Consequently, general contact was defined as an interface boundary condition between the SAS and dura mater to recreate the actual condition of this layer. An ABAQUS explicit dynamic analysis was performed along with a convergence study and the shear strain in the brain was studied. The material properties shown in Tables 1 and 2 were used.

To estimate and to further identify realistic material properties of the SAS, 12 different cases (corresponding to the Young's modulus ranging from 10^2 to 10^5 Pa) were studied using the same load and boundary conditions, and the properties of the skull and brain given in Table 1 and Table 2. The solutions associate with the maximum shear strain in the brain were determined at three arbitrary nodes corresponding to different locations in the brain (Nodes 3504, 3516, 1791) and were comparable to the 2% to 3% shear strains obtained from the experimental studies of Sabet *et al.* (2007) and Bayly *et al*. (2005), as shown in Fig. 3. The results indicated that a Young's modulus range of 1000-1500 Pa was associated with a strain range that is within the 2% to 3% shear strain values reported by Sabet *et al*. (2007). However, a modulus of 1150 Pa was selected for these analyses since it gave the best approximation to the experimental results. The nodal shear strain pattern of the brain is shown in Fig. 3. This model suggested that a modulus of elasticity of greater than 1500 Pa for the SAS should be disregarded otherwise the SAS will be too stiff to damp and protect the brain.

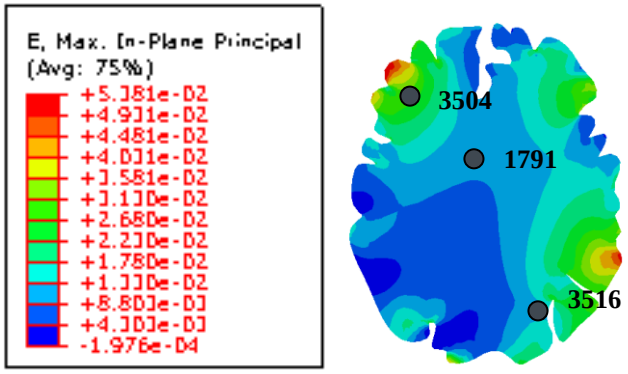

Fig. 3 Shear strain contour for a transverse model- nodal solution

2.2 The 3D head model

Several studies have suggested that a strain threshold of 10%-15% in the brain would indicate the onset of concussions leading to mild TBI, Bayly *et al.* (2005) and Meaney *et al.* (1995). In this section, the strain in the brain of a 3D head model is used to quantify the relationship between the magnitude of an external impact load to the head, leading to concussion or mild TBI. The validated material properties of the subarachnoid space determined in the previous sections were employed in the 3D model of the head used in this analysis.

The 3D head-neck model was created using the same MRI images of the female adult patient in her 50's as mentioned above. The details of the geometry and the dimensions were again determined using eRAD/Image Medical Practice builder 1-2-3 software. To create the 3D model of the head, initially transverse, sagittal and lateral planes of the head were defined, and many cross sections from each plane were imported into the ABAQUS/CAE sketch modules. Each cross-section was measured and the data was used to create the same section in ABAQUS/CAE. From cross sections that were imported into ABAQUS sketch modules, Solid Loft was used to create the left portion of the white mater of the brain. Due to the complexity of the white mater the model was then simplified using the MRI images and a simplified model of the white mater was used as a base model for the construction of the whole brain Fig. 4. Gray mater, the SAS, dura mater and the skull were created using the offset option of the sketch modules, and then different layers of the head were assembled to create a completed head model as shown in Fig. 4 and Fig. 5. The model of the face was then created using the same method that was used for the white mater, and the head-neck layer was subtracted from the 3D model of the face before all the layers were assembled as one to create the complete head model Fig. 5c. This was then used to create the FE model Fig. 5d. The model was then meshed using three-dimensional continuum elements (C3D10M) for all different sections. The SAS was also meshed using 3D stress elements (C3D4) with the total number of 3043 elements. The neck was modeled using the De Jager *et al.* (1994) approach, their model includes rigid head and vertebrae, connected by linear viscoelastic intervertebral joints and nonlinear elastic muscle elements.

ABAQUS6.10-EF1 was used as the pre and post processors, and an ABAQUS explicit dynamic analysis was performed. To reduce computational time, only half of the model was subjected to the displacement using symmetry boundary conditions. A convergence study was then performed to

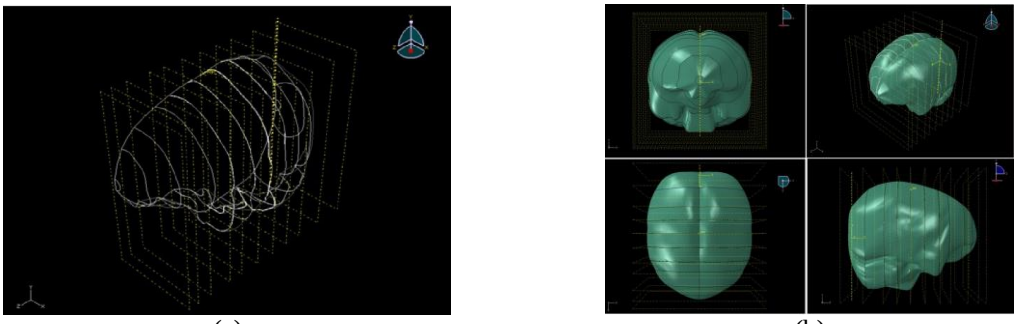

(a) (b)

Fig. 4 **(**a) Contours of lateral cross sections of the left side of the brain, and (b) the completed white mater model

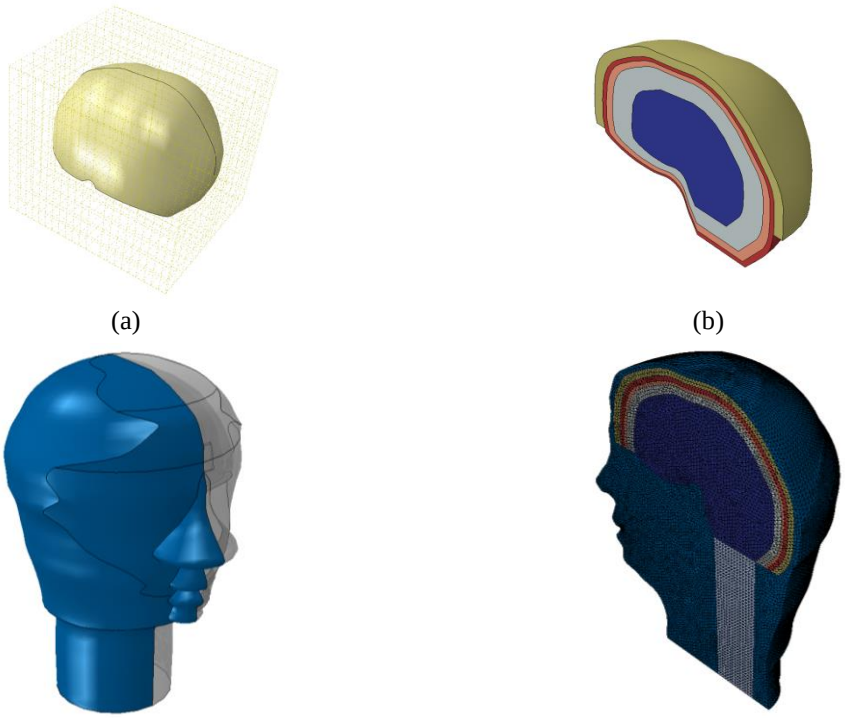

(a) (b)

(c) (d)

Fig. 5 Steps to complete the 3D head model; (a) the white mater, (b) the white mater, gray mater, SAS, dura and the skull model, (c) the head and neck model; and (d) the FE model of the head-neck

study the associated strains in the brain.

The material property of the brain was assumed to be isotropic and linear viscoelastic. All other components were assumed to be linear, isotropic and elastic. Tables 1 and 2, tabulate the material properties of the different components used in the 3D head model. However, the material properties of the SAS region used were those identified in the previous section, along with material properties documented by Zhang *et al.* (2001) and Zhang *et al.* (2002) and Takhounts *et al.* (2008).

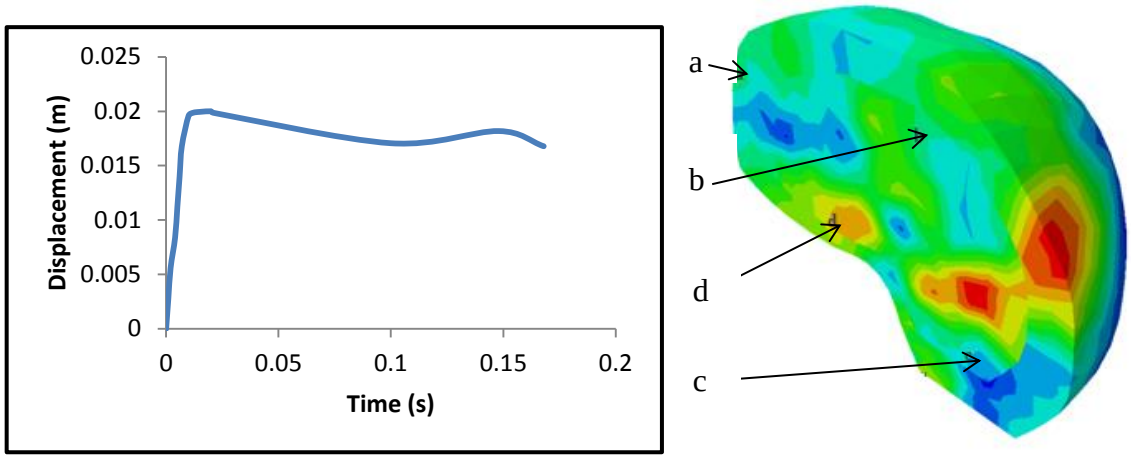

(a) (b)

Fig. 6 **(**a) Input boundary condition for the 3D head model Feng *et al.* (2010), and (b) the four material locations (a, b, c and d) in the model

The model was validated against an experimental study by Feng *et al*. (2010) where a human subject's head dropped 2 cm under its own weight and came in contact with a rubber band that was used to stop its fall. Displacement data were then obtained from this mild frontal head angular acceleration of the head and the impact with the rubber band. A tagged magnetic resonance imaging method was used to measure in vivo relative displacements between the brain and the skull of the three adult human subjects in the study. This study therefore provided an important set of displacement measurements of the human brain during a mild frontal skull impact. The results of Feng *et al*. (2010) also showed that at four specific locations in the brain, there was a 1-3 mm displacement of these locations relative to the skull Fig. 7.

This validated 3D head-neck model was then used to study the strain in the brain when the head is subjected to a wide range of blunt impacts with these being known to last for approximately between 30-50 ms, Hardy *et al.* (1997) and Zhang *et al.* (2001a), and having displacement curves that can be approximated by a sine function, Hardy *et al.* (1997). The 3D finite element model was subjected to the 11 different impact cases, corresponding to the velocity impacts ranging from 2.5 mph to 27 mph. These impacts were applied to the frontal region of the head. The inferior section of the neck of the model was restrained, and symmetric boundary conditions were applied on the plane of symmetry of the model. The head/neck model and its boundary conditions and loading are shown in Fig. 9(b). From this data a series of curves corresponding to the maximum strain in the brain for each velocity impact was established and the time history of the maximum strain in the brain was plotted.

3. Result

3.1 Validation

To validate the 3D head model the experimental work of Feng *et al*. (2010) was simulated. The center of the brain's mass in the 3D head model was subjected to a displacement of 2 cm as was

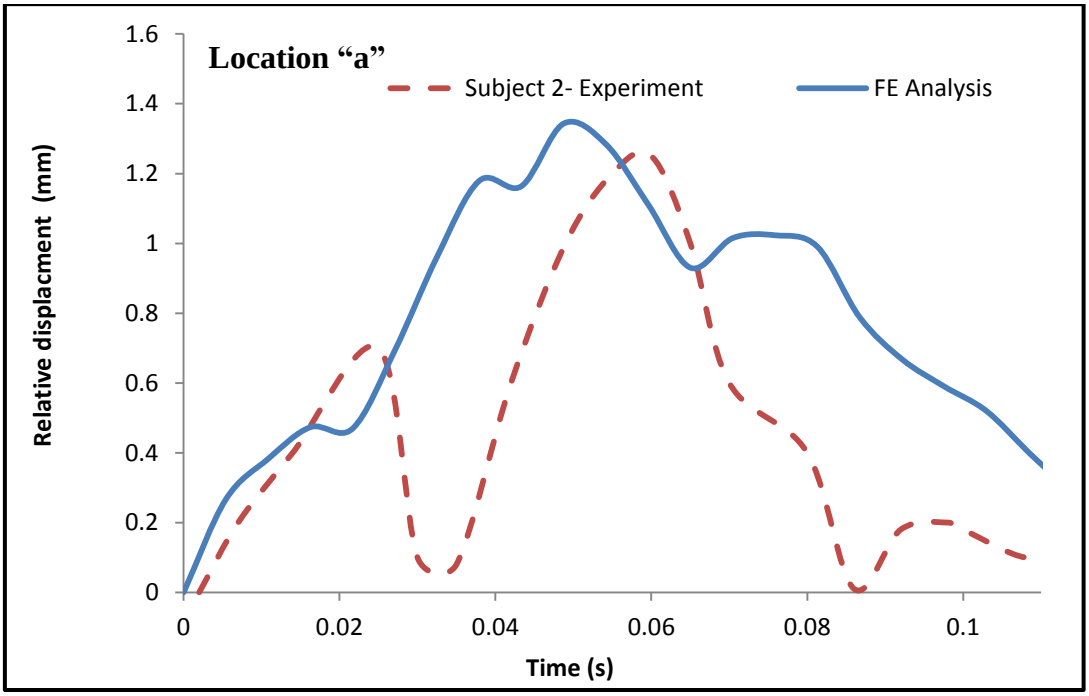

Fig. 7 Relative displacement between the skull and the brain at location “a”

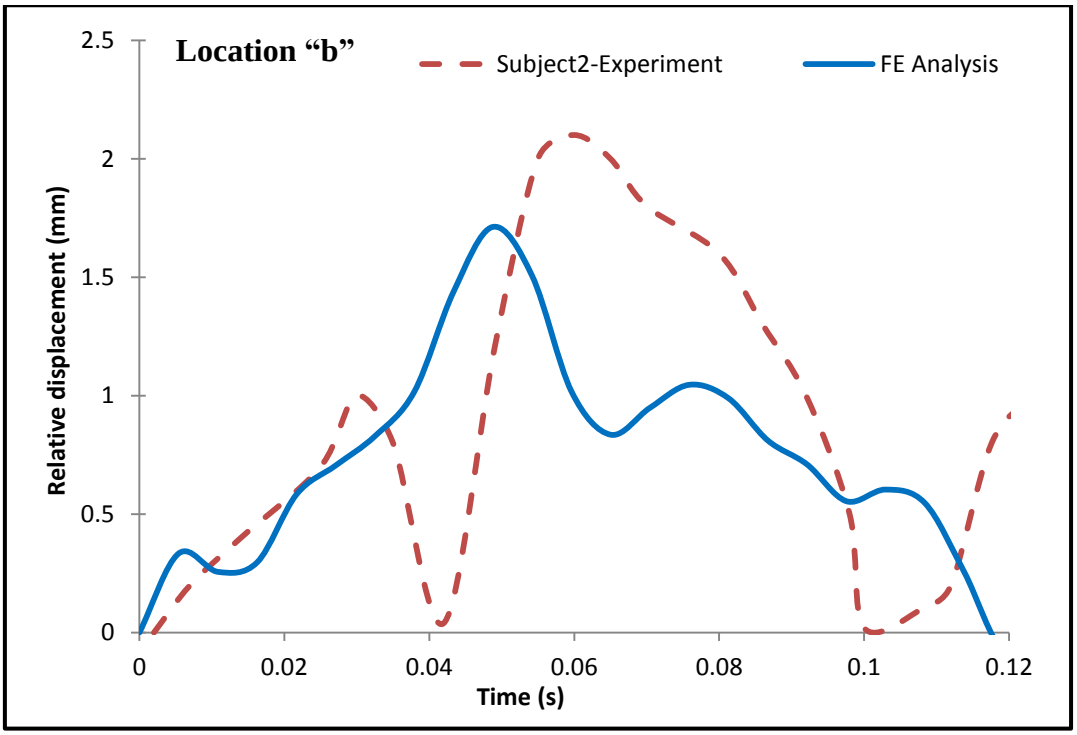

Fig. 8 Relative displacement between the skull and the brain at location “b”

the case in the experimental study Fig. 6(a). The model was restrained at the inferior point of the neck and only an in-plane (sagittal) rotation was allowed. An ABAQUS explicit dynamic analysis was performed and a relative displacement between the skull and brain was measured at the four material locations**.**

The nodal solutions of the relative displacement of four specific locations (a, b, c and d) within the brain and the skull were determined as shown in Fig. 6(b), and compared with the experimental results of Feng *et al.* (2010). Fig. 7 and Fig. 8 show that for the Young's modulus established by this work, the relative displacement between the brain and the skull is in good agreement with the displacement in subject 2 of the experimental study of Feng *et al*. (2010).

3.2 The blunt head impact

The validated 3D head model was used to study the strain in the brain when the head was subjected to a wide range of impacts that lasted between 30-50 ms, Hardy *et al*. (1997) and Zhang *et al*. (2001a), and which had displacement curves that were approximated using a sine curve, Hardy *et al*. (1997). From this model a series of curves for each velocity impact case was established.

The 3D finite element model was subjected to the 11 different impact cases, corresponding to the velocity impacts ranging from 2.5 mph to 27 mph. These impacts were applied to the frontal region of the head. The peak value of the displacement-time curve for a case where the head was subjected to an equivalent load corresponding to a 15 mph impact speed is shown in Fig. 9(a). The inferior section of the neck of the model was restrained, and symmetric boundary conditions were applied on the plane of symmetry of the model. The head/neck model and its boundary conditions and loading are shown in Fig. 9(b). In the first study, the frontal head of the 3D model was subjected to an impact corresponding to 2.5 mph (1.1 m/s), which is a displacement of 0.022 m in 20 ms. The model was then subjected to a series of impacts corresponding to 2.5 to 27 mph speeds and the brain strains were determined Fig. 10.

Fig. 10 shows the strain variation of the middle of the brain for all 11 cases. The results reveal that as the impact speed increases, the strain in the brain also increases. The maximum value of the

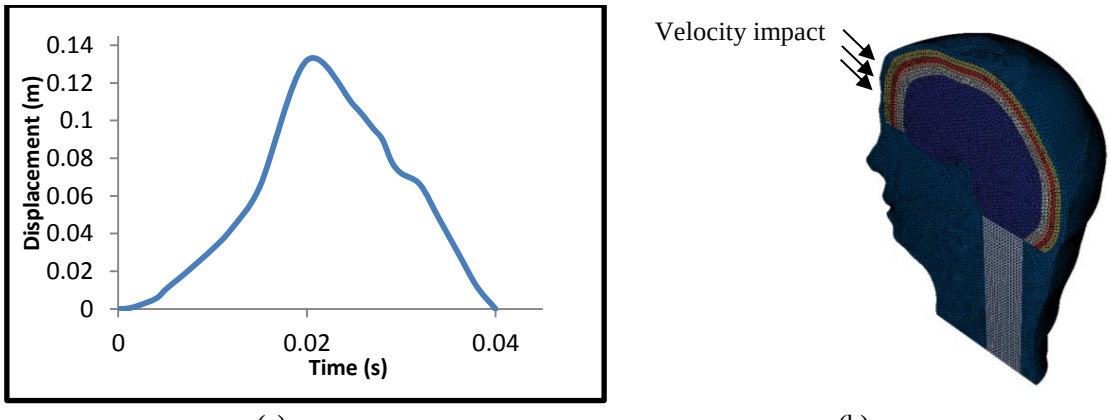

(a) (b)

Fig. 9 **(**a) Velocity impact profile corresponding to 15 mph (6.7 m/s) [9], and (b) the boundary conditions and loading applied to the frontal head of the 3D model

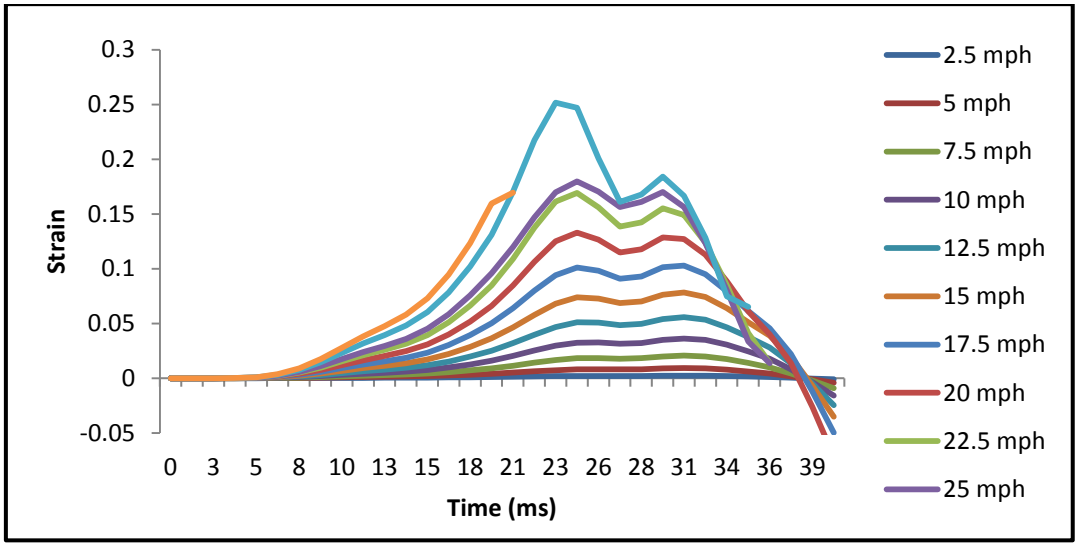

Fig. 10 Strain in the brain corresponding to 11 different cases of velocity impact

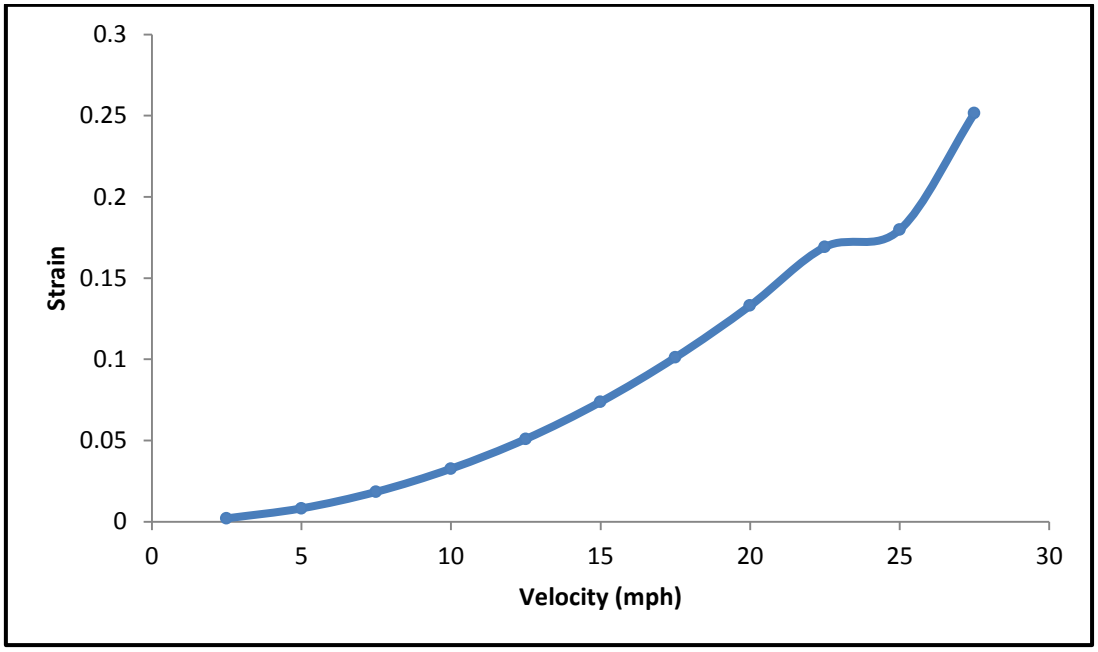

Fig. 11 Variation of the strain in the brain as a function of impact velocity to the head

strain corresponding to each case was determines and the maximum strain-velocity curve was plotted. This shows that if the applied impact velocity to the head changes from 2.5 to 27 mph, the maximum strain in the brain increases from 2% to 25%.

These analyses reveal that the maximum strain in the brain is quadratically proportional to the velocity impact on the frontal head as shown in Fig. 11. The relationship between strain and velocity can be define as $\varepsilon=(0.017V^2+0.0032V-0.012)$ where ε is the strain and V is the velocity of

the head in mph. Therefore, with increasing impact velocity, the likelihood of TBI increases quadratically.

4. Conclusions

The human head is the vulnerable body region that is most frequently associated with life threatening injuries; specifically traumatic brain injuries (TBI). Because of safety considerations, human and animal experimental studies are limited to mild impacts or accelerations. Therefore validated computer models are valuable tools for investigators to quantify the strain in the brain and the study of TBI. In this study the material properties of the SAS were investigated, since the literature cited values that were as much as three orders of magnitude different.

To identify a realistic range of the material properties of the SAS a 2D FE model was employed and analyzed using a wide range of the mechanical properties reported in the literature. In addition, the optimum material property for the SAS/trabeculae was determined based on the validation of the models with the experimental results of Sabet *et al.* (2007). The result indicated that the optimum elastic modulus of the trabeculae is 1150 Pa. This is consistent with the two previous studies of Saboori and Sadegh (2009 and 2010) where it was concluded that the trabeculae should be modeled as having a soft elastic modulus and be simulated as tension-only elements, since the trabeculae buckle with minimal compressive load.

It was further determined that the SAS material properties used by some investigators was too stiff and could lead to unreliable results. For example, if the material property of the trabecula reported by Zhang *et al*. (2006), $E=21.5\times10^6$ Pa, or Jin X *et al.* (2006), $E=59.8\times10^3$ Pa, is used the trabeculae would not buckle and the load or the impact would be transmitted directly to the brain. However, based on our previous histology and experimental work Saboori and Sadegh (2010, 2011) the soft tissue of the trabeculae was observed to buckle when the brain approaches the skull, thereby reducing the force transmitted to the brain. This indicates that the mechanical properties of the SAS reported by Zhang *et al*. (2006) and Jin *et al.* (2006) are not realistic.

In the second part of this study, an anatomically correct 3D model was created from the MRI of a human subject and was validated against the experimental study of Fang *et al.* (2010). Then the displacements in the brain were compared to the relative displacement between the brain and the skull as observed in an experimental study. The nodal solutions of the strain in the brain for two material locations (shown in Fig. 7 and Fig. 8) were determined and were found that, the relative displacement between the skull and the brain were in good agreement with the experimental study of Fang *et al.* (2010).

The experimental curves of Fang *et al.* (2010) shown in Fig. 7 and Fig. 8 indicate two peaks during the 168 ms period of the study, where the first peak, which occurs at about 40-60 ms, is associated with the maximum angular acceleration of the head, and occurs when the head of the subject hits the rubber band. Then once the elastic rubber band is stretched, it creates a rebound force pushing the head upward at which point the head of the subject separates from the rubber band followed by the head dropping back down again under its own weight. This is the moment when the second peak in the experimental result occurs. Note that in the model described in this paper, the rebound force of the rubber band, associated with the second peak, was not considered. Also it is important to note that the time lag after the first peak, between the experiment and the FEM results reported here, is due to the secondary force of the rubber and was also not considered in the FE model.

The result of the 3D head model validation indicated that the proposed Young's modulus in this study for the SAS is a reliable and appropriate value. The proposed value of *E* also suggested that the SAS material is soft and absorbs the brain's movement. This confirms the hypothesis about the functionality of the SAS (i.e., it acts as a damper and a shock absorber of the brain).

Finally, the validated 3D head model was subjected to a wide range of velocity impacts (2.5 to 27 mph) and a relationship between the applied velocities and the strain in the brain was established. The results reveal that the strain in the brain is quadratically proportional to the velocity impact. In addition, the results of this study further indicated that the material properties of the SAS play a significant role in transferring the load/impact to the brain and result in different types of TBI.

In the studies of Meany *et al*. (1995) and Bayly *et al.* (2005) it was shown that different types of TBI occur if the axon of the neuron nerve in the brain stretches more that 10%-15%. The myelin sheath around the axon nerve becomes damaged beyond repair because the nerve tissues are incapable of recovering and healing themselves. The analyses presented in this study reveal that the strain in the brain is related to the velocity impact and thereby different types of TBI. The result of this study also indicates that when the head is subjected to an impact corresponding to a velocity of 17-20 mph the strain in the brain is between, 10%-13%. For this range of impact speeds, the strain in the brain is less than the 15% threshold needed to cause traumatic brain injury (TBI) as cited in the literature, Meany *et al*. (1995) and Bayly *et al.* (2005). Therefore, it is concluded that if the head is subjected to an impact velocity of less than 20 mph the strain in the brain will be below the threshold for TBI.

Acknowledgements

This research was supported by the grant from the PSC-CUNY and the City University of New York.

References

Al-Bsharat, A.S., Hardy, W.N., Yang, K.H., Khalil, T.B., Tashman, S. and King, A.I. (1999), "Brain/Skull relative displacement magnitude due to blunt head impact: new experimental data and model", *Stapp Car Crash Conference*, **43**, 99SC22.

Bayly, P.V., Cohen, T.S., Leister, E.P., Ajo, D., Leuthardt, E. and Genin, G.M. (2005), "Deformation of the human brain induced by mild acceleration", *J. Neurotra.*, **22**(8), 845-856.

CDC (2011), www.cdc.gov.

De Jager, M., Sauren, A., Thunnissen, J. and Wismans, J. (1994), "A three-dimensional head-neck model: validation for frontal and lateral impacts", *Proceedings of the 38th Stapp conference and Society of Automotive Engineers*, SAE paper No. 942211.

Drew, W.E. (2004), "The contrecoup-coup phenomenon: a new understanding of the mechanism of closed head injury", *J. Neurocritical Care*, **1**, 385-390.

Feng, Y, Abney, T.M., Okamoto, R.J., Pless, R.B., Genin, G.M. and Bayly, P.V. (2010), "Relative brain displacement and deformation during constrained mild frontal head impact", *J. Royl. Soc*., **7**(53),1677-1688.

Frederickson, G.R. (1991), "The subdural space interpreted as a cellular layer of meninges", *The Anatomic. Rec*., **230**(1), 38-51.

Guo, P., Weinstein, A.M. and Weinbaum, S. (2000), "A hydrodynamic mechanosensory hypothesis for

brush border microvilli", *Am. J. Phys.*, **279**(4), F698-712.
Hardy, W.N., Foster, C.D., King, A.I. and Tashman, S. (1997), "Investigation of Brain Injury Kinematics: Introduction of A New Technique", Crashworthiness, Occupant Protection, BED 38 ASME, **225**, 241-254.
Jia, Li, Lei, Fang, Peter, Meyer, Hanspeter, E. Killer, Josef, Flammer and Albert, Neutzner (2014), "Anti-inflammatory response following uptake of apoptotic bodies by meningothelial cells", *J. Neuroinflam.*, **24**, 11-35.
Jin, X., Lee, J.B., Leung, L.Y., Zhang, L., Yang, K.H. and King, A.I. (2006), "Biomechanics response of the bovine pia-arachnoid complex to tensile loading at varying strain-rates", *Stapp Car Crash J.*, **50**, 637-649.
Kierszenbaum, L., Abraham (2007), *Histology and Cell Biology an Introduction to Pathology*, Second edition, Elsevier Health Sciences, NY, USA.
Killer, H.E., Laeng, H.R., Flammer, J. and Groscurth, P. (2003), "Architecture of arachnoid trabeculae, pillars, and septa in the subarachnoid space of the human optic nerve", *The British J. Ophthalmol.*, **87**(6), 777-781.
Killer, H.E., Jaggi, G.P., Flammer, J., Miller, N.R. and Huber, A.R. (2006), "The optic nerve: a new window into cerebrospinal fluid composition", *Brain J. Neouralogy*, **129**(4), 1027-1030.
Kleiven, S. and Hardy, W.N. (2002), "Correlation of an FE model of the human head with local brain motion-consequences for injury protect", *Stapp Car Crash J.*, **46**, 2002-22-0007.
Meaney, David, F., Douglas, H., Smith, David, I., Shreiber, Allisson, C., Bain, Reid, T., Miller, Doug, T., Ross and Thomas, A., Gennarelli (1995), "Biomechanics analysis of experimental diffuse axonal injury", *J. Neurotra.*, **12**(4), 689-695.
Rao, V. and Lyketsos, C. (2000), "Neuropsychiatric sequelae of traumatic brain injury", *J. Psychosom.*, **41**(2), 95-103.
Ruan, J.S., Khalil, T.B. and King, A.I. (1993), "Finite element modeling of direct head impact", *Stapp Car Crash Conference*, **37**, 933114.
Sabet, A., Christoforou, E., Zatlin, B., Genin, G.M. and Bayly, P.V. (2007), "Deformation of the human brain induced by mild Angular head acceleration", *J. Biomech.*, **41**(2), 307-315.
Saboori, P. and Sadegh, A. (2013), "Histology and morphology of the brain sub arachnoid trabeculae", *Medical Eng. Physics*.
Saboori, P. and Sadegh, A. (2009), "Effect of mechanical properties of SAS trabeculae in transferring loads to the brain", *Proceedings of the International Mech. Eng. Congress and Exposition*, (IMECE), BED/ASME, Lake Buena Vista Florida.
Saboori, P. and Sadegh, A. (2010), "Modeling of subarachnoid space and trabeculae architecture as it relates to TBI", *16th US National Congress of Theoretical and Appl. Mech.* (USNCTAM2010-887), State College Pennsylvania.
Saboori, P. (2011), "Mechanotransduction of head impacts to the brain leading to TBI: histology and architecture of subarachnoid space", Ph.D. Dissertation, The City University of New York, USA.
Schachenmayr, W. and Friede, R.L. (1978), "The origin of subdural neomembranes. I. Fine structure of the dura-arachnoid interface in man", *Am. J. Pathol.*, **92**(1), 53-68.
Takhounts, E.G., Ridella, S.A., Hasija, V., Tannous, R.E., Campbell, J.Q., Malone, D., Danelson, K., Stitzel, J., Rowson, S. and Duma, S. (2008), "Investigation of traumatic brain injuries using the next generation of simulated injury monitor (SIMon) finite element head model", *Stapp Car Crash J.*, **52**, 1-3.
Zhang, L., Yang, K.H., Dwarampudi, R., Omori, K., Li, T., Chang, K., Hardy, W.N., Khalil, T.B. and King, A.I. (2001a), "Recent advances in brain injury research: a new human head model development and validation", *Stapp Car Crash J.*, (45), 369-394.
Zhang, L., Yang, K.H. and King, A.I. (2001b), "Biomechanics of neurotrauma", *Neurologi. Res.*, **23**, 144-156.
Zhang, L., Bae, J., Hardy, W.N., Monson, K.L., Manley, G.T., Goldsmith, W., Yang, K.H. and King, A.I. (2002), "Computational study of the contribution of the vasculature on the dynamic response of the brain", *Stapp Car Crash J.*, **46**, 145-164.

Zoghi, M. and Sadegh, A. (2010), "Equivalent fluid model for CSF and SAS trabeculae using Head/Brain damping", *Int J. Biomed. Eng. Tech.*, **4**(3), 195-201.
Zoghi, M. and Sadegh, A. (2009), "Global/Local head models to analyze cerebral blood vessel rupture leading to ASDH and SAH", *Int. J. Comput. Meth. Biomech. Biomed. Eng.*, **12**(1), 1-12.

CC